Quaternary Science Reviews 126 (2015) 112–125

Contents lists available at ScienceDirect

Quaternary Science Reviews

journal homepage: www.elsevier.com/locate/quascirev

Vegetation and climate history in arid western China during MIS2: New insights from pollen and grain-size data of the Balikun Lake, eastern Tien Shan

Yongtao Zhao [a], Cheng-Bang An [a, *], Limi Mao [b], Jiaju Zhao [a], Lingyu Tang [b], Aifeng Zhou [a], Hu Li [a], Weimiao Dong [a], Futao Duan [a], Fahu Chen [a]

[a] Key Laboratory of Western China's Environmental Systems (Ministry of Education), College of Earth and Environmental Sciences, Lanzhou University, Lanzhou 73000, China
[b] Nanjing Institute of Geology and Palaeontology, Chinese Academy of Sciences, Nanjing 210008, China

ARTICLE INFO

Article history:
Received 17 December 2014
Received in revised form
20 August 2015
Accepted 26 August 2015
Available online xxx

Keywords:
Vegetation
Climate
Pollen analysis
Grain size
Last glacial maximum
Balikun lake
Western China

ABSTRACT

Marine Isotope Stage (MIS) 2 is mostly a cold period encompassing the Last Glacial Maximum (LGM), but the regional expression of MIS2 in arid areas of China is not well known. In this paper, we use high-resolution lacustrine pollen and grain-size records from Balikun Lake to infer vegetation, lake evolution, and climate in arid western China during MIS2. Our results suggest that: 1) the regional vegetation around Balikun was mainly dominated by desert and/or desert-steppe, and Balikun Lake was relatively shallow and experienced high aeolian input during MIS2; 2) distinctive runoff from mountain glacial meltwater in the eastern parts of the Balikun basin caused a high relative abundance of *Artemisia* pollen during the LGM (26.5–19.2 cal kyr BP), while simultaneously the desert areas expanded as indicated by the high abundance of desert shrubs (e.g., Elaeagnaceae, Rhamnaceae, *Hippophae*). This cold and dry LGM climate triggered a substantial lowering of lake level; 3) an extremely cold and dry climate prevailing from 17.0 to 15.2 cal kyr BP, correlated with Heinrich event 1 (H1), would explain the low vegetation cover found then; and 4) the warm and humid Bølling/Allerød interstadial (BA: *ca.* 15–*ca.* 13 cal kyr BP) is clearly recorded in the Balikun region by the development of wetland herb communities (e.g., Poaceae, Cyperaceae, *Typha*), and the lake level rose due to increased runoff. Our results challenge the traditional view of cold and wet climatic conditions and high lake levels in arid western China during the LGM, and we propose that changes in local temperature modulated by July insolation was an indispensable factor in triggering vegetation evolution in the Balikun region during MIS2.

1. Introduction

Marine Isotope Stage (MIS) 2 (*ca.* 29–*ca.* 14 cal kyr BP, Lisiecki and Raymo, 2005) is an interval of mostly cold climate conditions along with low sea level and vast ice masses in Europe and North America (Mix et al., 2001; Clark et al., 2009), which led to a reorganization of major atmospheric and hydrological systems in the Northern Hemisphere (Bigelow et al., 2003; Mithen, 2006; Shakun and Carlson, 2009). Detailed vegetation and lake responses to such remarkable climate changes during MIS2 have, to date, been poorly documented, especially in the arid central Asian region. For example, lacustrine records from western and northern parts of arid central Asia (e.g., Caspian Sea (Kislov and Toropov, 2011; Kislov et al., 2012, 2014); Aral Sea (Mamedov, 1991; Boomer et al., 2000); Lake Baikal (Prokopenko et al., 2005; Kostrova et al., 2014; Nara et al., 2014); Kotokel Lake (Müller et al., 2014)) show a regionally coherent pattern of lower-than-present lake levels during MIS2, and palynological evidence suggests that periglacial tundra steppe and sparse herbaceous vegetation with low pollen accumulation rates dominated the high latitudes of arid central Asia (Simakova, 2006; Markova et al., 2009; Shichi et al., 2013), indicating a cold and dry climate. However, the climate of arid western China during MIS2 is much debated (e.g., Li, 1990; Qin and Yu, 1998; Yu et al., 2000, 2003; Herzschuh et al., 2005; Herzschuh, 2006; Ju et al., 2007; Wünnemann et al., 2007; C. Luo et al., 2009; Yang and

* Corresponding author. Key Laboratory of Western China's Environmental Systems (Ministry of Education), Lanzhou University, Lanzhou 730000, Gansu, China.
E-mail address: cban@lzu.edu.cn (C.-B. An).

http://dx.doi.org/10.1016/j.quascirev.2015.08.027
0277-3791/

Scuderi, 2010; Yang et al., 2011; An et al., 2013; Yan and Wünnemann, 2014). Based on an integrated analysis of multi-archives such as lake-level, pollen, and stratigraphy, Li (1990) suggests that the climate during the LGM in arid western China was cold and wet, accompanied by high lake-levels corresponding with a glacial advance period. Yu et al. (2000) and Ju et al. (2007) also show that precipitation and effective moisture increased during the LGM (*ca*. 26.5—*ca.* 19/18 cal kyr BP, Clark et al., 2009) likely due to the southward migration of the westerlies and low evaporation caused by low air temperatures. However, palaeoclimatic studies from lakes (e.g., Rhodes et al., 1996; Herzschuh et al., 2005; Mischke et al., 2005; Wünnemann et al., 2007; An et al., 2013; Yan and Wünnemann, 2014), deserts (e.g., Sun et al., 1998; Dong, 2002; Chen et al., 2014), loess (Li et al., 2011), and general circulation modelling (GCM) (Li and Morrill, 2013) suggest a cold and dry climate during the LGM in arid western China.

This discrepancy is probably caused by: 1) the absence of MIS2 sediments due to erosion (e.g., Rhodes et al., 1996; Zhao et al., 2013); 2) the lack of robust age control (e.g., Shi et al., 1990; C. Luo et al., 2009); and/or 3) low temporal resolution (e.g., Li et al., 1989; An et al., 2013). Moreover, the low evaporation rate invoked to explain the high lake levels appears to be less effective than the effect of reduced precipitation (Li and Morrill, 2013). The chronological issues and inadequate pollen data during the LGM may have compromised the palaeoclimatic interpretation and also likely introduced errors into the model output because of the poorly defined boundary conditions. A well-dated pollen record in this area is therefore needed to evaluate better the vegetation and climate history during MIS2.

Previous palynological studies in the Balikun area of eastern Xinjiang are limited. Tao et al. (2010) established a pattern of pollen distribution from surface sediments, which may help in the interpretation of postglacial and Holocene pollen deposits and the reconstruction of climate changes. An et al. (2013) reconstructed the vegetation history of MIS2 at a relatively low temporal resolution. In this study, we employ a well-dated core (BLK11A) recovered from Balikun Lake to reconstruct the climate during MIS2, with an emphasis on the LGM. Ordination analysis of pollen data is used to extract primary variables correlated with the distribution of pollen samples and pollen taxa so as to infer the regional vegetation history. End-member modelling analysis (EMMA) of grain-size data is used to explain the sediment transport processes and thus to characterize lake evolution and typical depositional environments. This study not only improves our understanding about vegetation and climate changes during MIS2 in arid central Asia but also yields important data which can be used to test GCM output of past climate change.

2. Regional setting

2.1. Site description

The Balikun basin is a faulted plateau basin situated in the eastern part of Xinjiang. It lies between the Balikun Mountains to the south and the Moqinwula Mountains to the north (Fig. 1a and b; Han et al., 1989). Balikun Lake (43°36′ – 43°45′ N; 92°42′ – 92°54′ E; 1575 m a.s.l) is located in the west of the Balikun basin (Fig. 1a and b). It is a hydrologically closed inland lake and has been since the Late Pleistocene (Ma et al., 2004) with a peculiar wetland-arid ecosystem. A number of alluvial fans are distributed in the western basin, and the Dahe River originates on the northern slopes of the Balikun Mountains, runs along the Balikun steppe to the west and finally discharges into Balikun Lake (Fig. 1b). Abundant pollen deposits are transported into the lake by this river, making it possible to reconstruct the regional vegetation history.

2.2. Modern climate and vegetation

Meteorological data for Balikun Lake were obtained by extrapolating data from the Balikun meteorological station (Fig. 1b), and gives mean monthly temperatures of −18.1 °C for January and 17.1 °C for July. Mean annual precipitation is less than 210.9 mm, and 54% of the rainfall occurs between June and August, with very high potential evaporation of 1602.7 mm (Fig. 1c), reflecting the typical continental climate of our study area (Zheng, 1997; Wang and Dou, 1998).

According to the regional vegetation survey by the Integrative Investigative Team of Xinjiang (1978), modern vegetation between 2800 and 2900 m a.s.l. in the Balikun basin is dominated by alpine meadow (mainly *Kobresia capilliformis*), and between 2100 and 2800 m a.s.l. by coniferous forest (*Larix sibirica, Picea schrenkiana*). Desert steppe (*Stipa glareosa*, *Festuca sulcate, Allium polyrrhizum*) and desert shrubs occur on the piedmont. The vegetation in the western and eastern parts of the Balikun basin is quite different in terms of both composition and cover. Desert Amaranthaceae and Asteraceae with a low vegetation cover are distributed on the western side of the basin (Fig. 2a and b), while well-developed vegetation (mainly *Artemisia* and Poaceae) with a high cover is distributed on the eastern side of the basin (Fig. 2c and d).

3. Materials and methods

3.1. Sediment core and dating

A 62.53-m-long core (BLK11A) was taken from the centre of Balikun Lake in June 2011 using a Kullenberg Uwitech Coring System. In this study, we focus on a segment of the core between 294 and 720 cm to study climate change during MIS2 and the last deglaciation. The core was subsampled at 1-cm intervals in the laboratory and then freeze-dried. The chronology framework of the core was established by nine accelerator mass spectrometry (AMS) ^{14}C dates measured by Beta Analytic Inc., USA on various fractions including bulk clay, charcoal, charred seeds (*Ruppia*), and plant macrofossils.

3.2. Grain-size analysis and end-member modelling

Samples of sediment grain-size distribution were measured at 1-cm intervals in the Laboratory of Western China's Environmental System, Lanzhou University to obtain a high-resolution record of sedimentation dynamics. Samples were pre-treated with 10% H_2O_2 and 10% HCl to remove dissolvable salts and organic matter. The remaining material, generally within the size range of terrestrial debris according to Peng et al. (2005), was dispersed by sonication prior to measurement. The measurement was conducted using the Malvern Co. Ltd. Mastersizer 2000 laser diffraction particle-size analyser. Error in the average grain size was less than 2%.

End-member modelling analysis (EMMA), an eigenspace decomposition essentially based on polytope expansion with different scaling procedures, was conducted to extract genetically meaningful end-member grain-size distributions (i.e., loadings) and their percentages in each sample (end-member composition, i.e., scores). These end members are believed to represent the sediment transport processes and thus are characteristic of the typical depositional environments (Weltje, 1997; Weltje and Prins, 2003; Yu, 2015). The 10th quantile ($l = 0.1$) was applied in the weight transformation after Dietze et al. (2012, 2013), which yielded the best unmixing and modelling results compared to other model configurations.

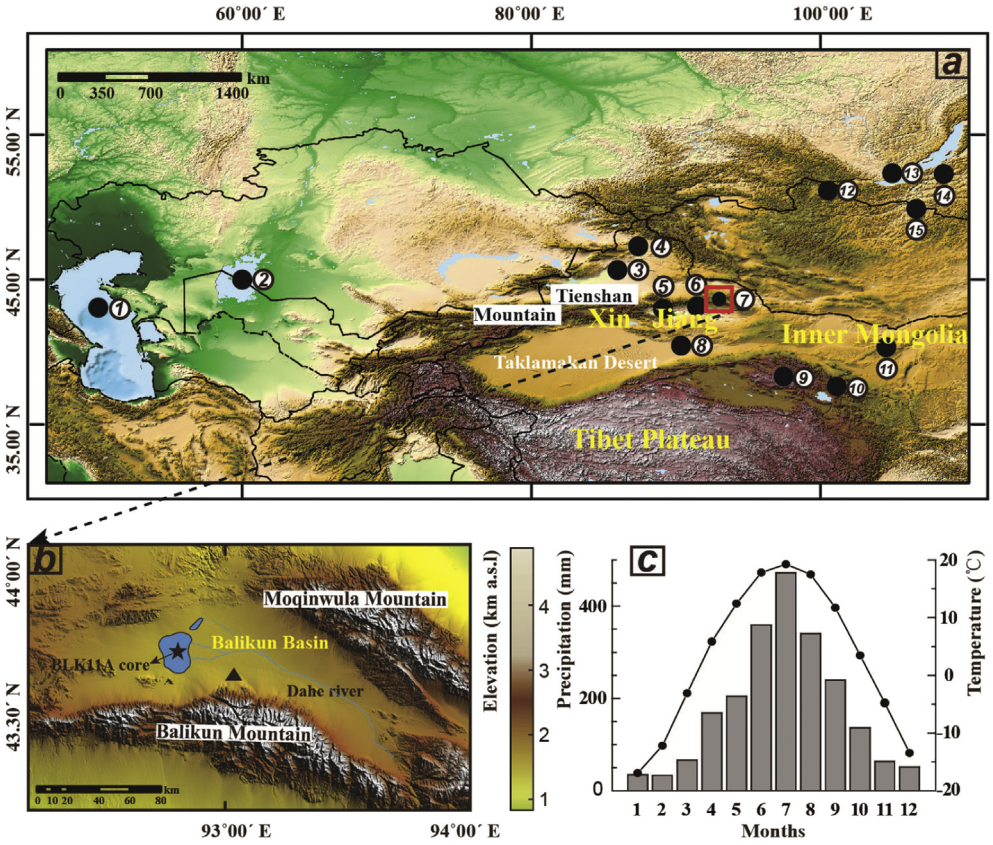

Fig. 1. a: Location of our study area in the red rectangle and other palaeoclimate proxy records cited in the text (1, Caspian Sea; 2, Aral Sea; 3, Manas Lake; 4, Wulungu Lake; 5, Bosten Lake; 6, Aydian Lake; 7, Balikun Lake (this study); 8, Lop Nur; 9, Hala Lake; 10, Luanhaizi; 11, Baijian Lake; 12, Hovsgol Lake; 13, Lake Baikal; 14, Kotokel Lake; 15, Gun Nuur); b: the core BLK11A site (black star) in Balikun Lake, and the Balikun meteorological station (black triangle); c: mean monthly temperature and precipitation from Balikun meteorological station for AD 1958–2003. (For interpretation of the references to colour in this figure legend, the reader is referred to the web version of this article.)

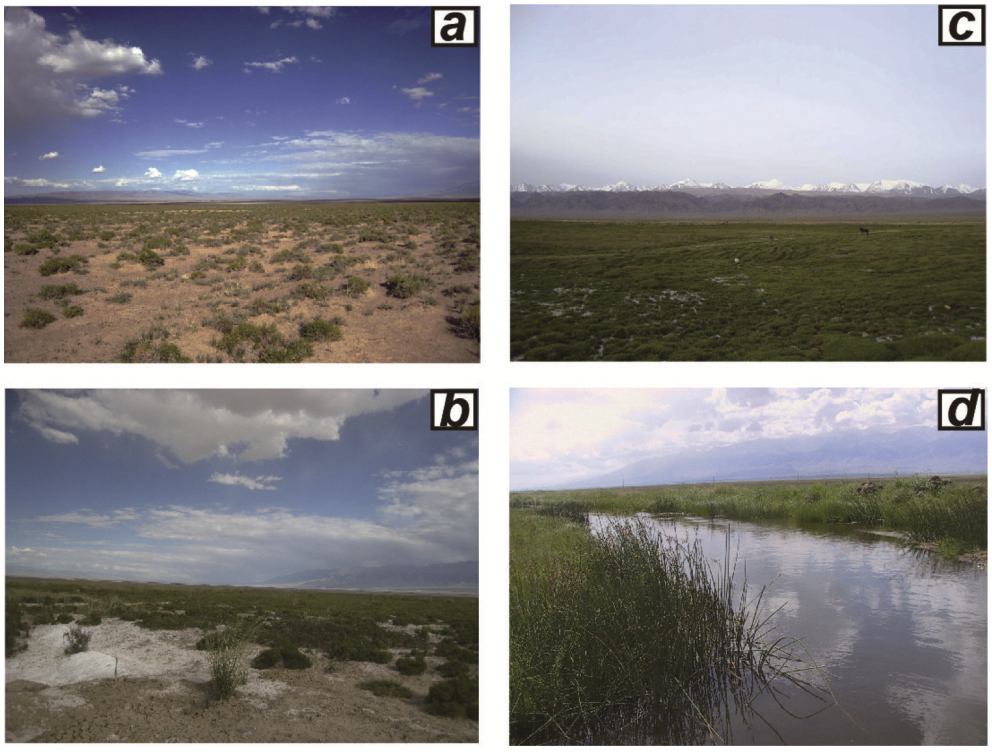

Fig. 2. Pictures showing modern vegetation communities on the western side of Balikun Lake with low cover (a, b) and the eastern side with high cover (c, d).

3.3. Pollen analysis

In total, 78 samples were collected from the sediment core at 4–6 cm intervals for pollen analysis. Palynomorph extraction followed the routine process described by Fægri and Iversen (1989). One marker tablet with a known number (27637) of *Lycopodium* spores was added prior to the chemical treatment in order to calculate pollen concentrations. Pollen identification follows pollen atlases for the arid and semi-arid areas of China (e.g., Xi and Ning, 1994; Wang et al., 1995). All of the palynomorphs were counted under a Nikon light microscope at 400× magnification. At least 300 grains of terrestrial plant pollen from each sample were counted for principal component analysis (PCA). Pollen diagrams were generated using Tilia v2.02 (Grimm, 2004). Pollen zones and subzones were assigned using the stratigraphically constrained cluster analysis program CONISS (Grimm, 1987, 2004).

The PCA was conducted using CANOCO v4.52 (ter Braak and Šmilauer, 2003). A total of 126 samples was analysed, including 78 pollen samples from core BLK11A in this study, and nine surface-sediment samples (An et al., 2013) and 39 mid-Holocene (*ca.* 8.0–*ca.* 5.0 cal kyr BP) pollen samples (Tao et al., 2010) from another core from Balikun Lake, BLK06E. Prior to the ordination analysis, detrended correspondence analysis (DCA) was performed to determine whether a linear or unimodal model was appropriate. The results of the DCA with a maximum gradient length of 1.40 (<3.0 standard deviations) suggested that a linear model was appropriate for the pollen assemblages. A linear unconstrained model PCA was then conducted to identify the factors controlling the composition of pollen samples and pollen taxa; the length of each pollen vector indicates how well the values of that type are approximated in the ordination diagram.

4. Results

4.1. Lithology and chronology

The core is mainly composed of clayey silt, occasionally intercalated with thin layers of clay and/or sand. The details of the lithology are as follows: 294–335 cm, grey-black silt; 335–480 cm, green-grey clay; 480–548 cm, grey-green sand; 548–595 cm, grey-black silty clay; 595–662 cm, grey clayey silt with bands of pale orange clay; 662–706 cm, grey clayey silt; 706–709 cm, grey silt with pieces of gypsum; 709–720 cm, grey clay (Fig. 3a).

Two charred *Ruppia* seeds, used for radiocarbon dating, have $\delta^{13}C$ values of −10.1‰ and −16.7‰ (Table 1), matching results from Sugan Lake (Zhou et al., 2009) and Qinghai Lake (Z.S. An et al., 2012). The ^{14}C-age of bulk clay at a depth of 565 cm agrees well with the charred seeds at almost the same depth (569 cm), indicating a relatively small reservoir age. A previous study shows that the magnitude of the reservoir effect in this lake is 790 years (C.B. An et al., 2012; 2013). After subtracting 790 years, all of the ages were converted to calendar years using Calib 7.0 software (Reimer et al., 2013) (Table 1). Linear interpolation or extrapolation between dates was used to create the age-depth model (Fig. 3b). The theoretical resolution during MIS2 is 50–250 years per sample.

4.2. Grain-size data

Unmixing of detrital grain-size distributions yielded an optimal model with three end-members (EMs) explaining 94.2% of the total variance (mean r^2 between the original and modelled data generally >0.65 ($p < 0.01$)). EMs 1, 2, and 3 explain 38.6%, 18.2%, and 43.0%, respectively. Grain-size distributions of 33 surface-sediment samples collected from lakes, rivers, and aeolian deposits were used to explain the sediment transport processes (Fig. 4) and the variances of the EMs in the core BLK11A (Fig. 8).

EM 1 shows a narrow peak in the very fine silt (mode at *ca.* 10 μm); its distribution mode is similar to that of modern lake surface-sediment samples and is generally high in subzone PB-4 (29.1–26.5 cal kyr BP) and subzone PA-2 (12.6–10.0 cal kyr BP). EM 1 is thought to represent sediments from a low-energy environment under calm water conditions. The abundance of this type in the sediment core indicates a depositional environment and lake depth similar to that of today.

EM 2 has an intensive range from 10 to 100 μm with a peak at *ca.* 60 μm, with a high level in subzone PB-2 and PB-3 (26.5–17.0 cal kyr BP) and PA-1 (10.0–8.9 cal kyr BP). Analysis of modern aeolian deposits shows that two main types exist around the Balikun region. The well-sorted Type 1 with one peak represents long-distance transportation, while the poorly-sorted Type 2 with three peaks is probably transported from nearby surfaces by strong winds. EM 2 has a similar distribution mode to a mixture of Type 1 and Type 2, and it indicates the strength of the aeolian dust or wind.

EM 3 shows a broad mode in the medium and coarse sand with a maximum at *ca.* 100 μm, and a second, but smaller peak at ca. 600 μm. It contributes to the sample compositions (i.e., scores) mainly in subzone PA-3 (15.2–12.6 cal kyr BP) and the coarse sediments in subzone PB-1 (17.0–15.2 cal kyr BP). Comparing it with modern samples collected from river sand and the palaeo-river channel, EM 3, with its typical three-stages of rolling, jumping, and suspension, is interpreted as being deposited by high-energy fluvial transport.

4.3. Pollen data

4.3.1. Modern pollen samples

Modern pollen samples, including nine surface-sediment samples from Balikun Lake and 37 topsoil samples from different vegetation communities in the vicinity of the lake, are discussed elsewhere (Tao et al., 2010; An et al., 2013). Here, we reconstruct the average values of the main pollen assemblages for every vegetation community (Fig. 5) to explain better the fossil pollen and therefore to reconstruct the vegetation and climate during MIS2. We find huge discrepancies in the dominant vegetation types in the different parts of the Balikun basin (especially the east and west): Amaranthaceae is the key family in the desert on the west side of the Balikun basin, while *Artemisia* comprises a significant proportion of the desert-steppe and steppe surrounding the lake as well as in the river meadow, alpine meadow below the conifer forest, and desert. Poaceae mainly develops in some low-lying areas (river meadow and reed bush) where sufficient water was provided by runoff in the eastern part of Balikun basin.

4.3.2. Fossil pollen from core BLK11A

The identified pollen grains comprise 40 taxa (families/genera). Arboreal trees are mainly represented by *Pinus*, *Picea*, *Ulmus*, *Carpinus*, *Betula*, and *Salix*; shrubs and dwarf-shrubs include Amaranthaceae (e.g., *Anabasis brevifolia*, *Eurotia ceratoides*), *Ephedra*, *Nitraria*, Elaeagnaceae, Rhamnaceae, Tamaricaceae, Apoaceae, and Zygophyllaceae. Major herb pollen types are *Artemisia*, Asteraceae, Poaceae, Fabaceae, Cyperaceae, Ranunculaceae, Saxifragaceae, *Polygonum*, *Thalictrum*, and Caryophyllaceae. There are also some aquatic pollen types such as *Typha* and *Ruppia*. Details of the two pollen zones and seven subzones are described below and shown on the pollen diagram (Fig. 6).

4.3.2.1. Pollen zone PB (720–520 cm, 29.1–15.2 cal kyr BP). Pollen assemblages of this zone are mainly dominated by *Artemisia* and Amaranthaceae, with a small portion of desert shrub pollen

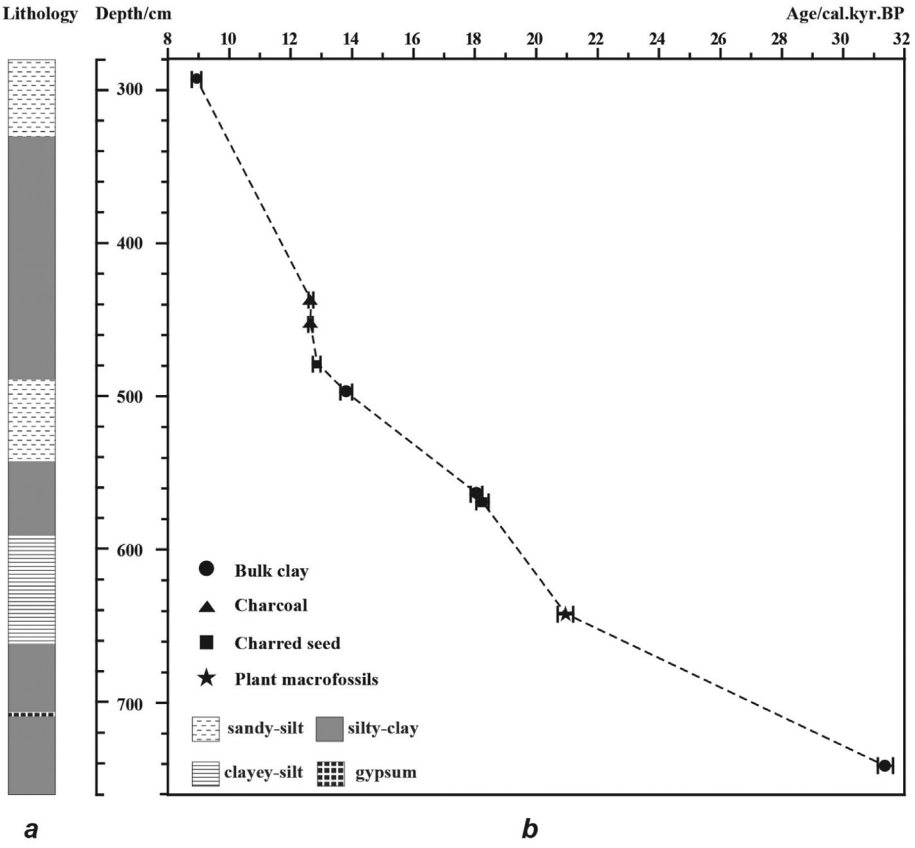

Fig. 3. Diagram showing (a) the lithology of the sampled section of the core BLK11A, and (b) an age-depth model.

Table 1
AMS radiocarbon dates and dated material from core BLK11A in Balikun Lake.

Laboratory code	Sample no.	Depth (cm)	Material dated	$\delta^{13}C$(‰ VPDB)	Conventional ^{14}C age (BP)	Calibrated ^{14}C age 2σ (cal. yr. BP)
345871	BLK11A-269	293	Bulk clay	−19.3	8860 ± 40	8779–9093
345873	BLK11A-400	437	Charcoal	−11.6	11520 ± 50	12587–12732
376479	BLK11A-415	453	Charcoal	−11.3	11480 ± 40	12576–12715
377642	BLK11A-439	479	Charred seeds	−16.7	11770 ± 40	12727–12974
345874	BLK11A-456	497	Bulk clay	−22.9	12750 ± 50	13619–14003
345875	BLK11A-519	565	Bulk clay	−21.0	15630 ± 60	17867–18246
377643	BLK11A-523	569	Charred seeds	−10.1	15820 ± 60	18045–18452
345881	BLK11A-591	642	Plant macrofossils	−11.8	18150 ± 70	20695–21202
345876	BLK11A-680	741	Bulk clay	−22.0	28400 ± 140	31131–31623

(e.g., Elaeagnaceae, Rhamnaceae, *Hippophae*), while wetland herbs (e.g., Poaceae, Cyperaceae, *Typha*) are relatively rare. Notably, this zone is characterized by a high percentage of *Artemisia* (*ca.* 50%), while the pollen concentrations are relatively low (*ca.* 5×10^3 grains/g).

4.3.2.2. Subzone PB-4 (720–695 cm, 29.1–26.5 cal kyr BP). Amaranthaceae and *Artemisia* are the dominant pollen components of this zone, accounting for 39.9% and 37.3% on average, respectively. *Ephedra* increases from 3.5% to 15.9%. Poaceae (4.8%) and Asteraceae (2.3%) are relatively higher than in the other subzones, and there is still a small proportion of *Betula* and *Juglans* pollen. *Typha* pollen constitutes 11.7% in the early part of the subzone, but decreases to nearly zero at approximately 695 cm. The pollen concentration decreases sharply from 27.6×10^3 to 1.6×10^3 grains/g.

4.3.2.3. Subzone PB-3 (695–595 cm, 26.5–19.2 cal kyr BP). A notable feature of this zone is the increased desert shrub pollen (e.g., Elaeagnaceae, Rhamnaceae, Apoaceae, Zygophyllaceae). *Artemisia* (55.1%) increases markedly, while Amaranthaceae falls to 28.0%. *Ephedra* and Poaceae decrease to 1.3% and 3.1% on average, respectively. The mean pollen concentration is relatively low (5.3×10^3 grains/g).

4.3.2.4. Subzone PB-2 (595–548 cm, 19.2–17.0 cal kyr BP). *Artemisia* and Amaranthaceae are still the dominant pollen components throughout this zone. *Artemisia* increases to 58.3%, higher than in the other subzones. The pollen concentration fluctuates from 1.9×10^3 to 13.1×10^3 grains/g.

4.3.2.5. Subzone PB-1 (548–520 cm, 17.0–15.2 cal kyr BP). *Artemisia* shows a clear decreasing trend (51.3% on average), while Asteraceae increases from 1.2% to 13.5%. The mean percentage of Amaranthaceae is 25.7%. The pollen concentration reaches its lowest value (1.4×10^3 grains/g, mean) in this subzone.

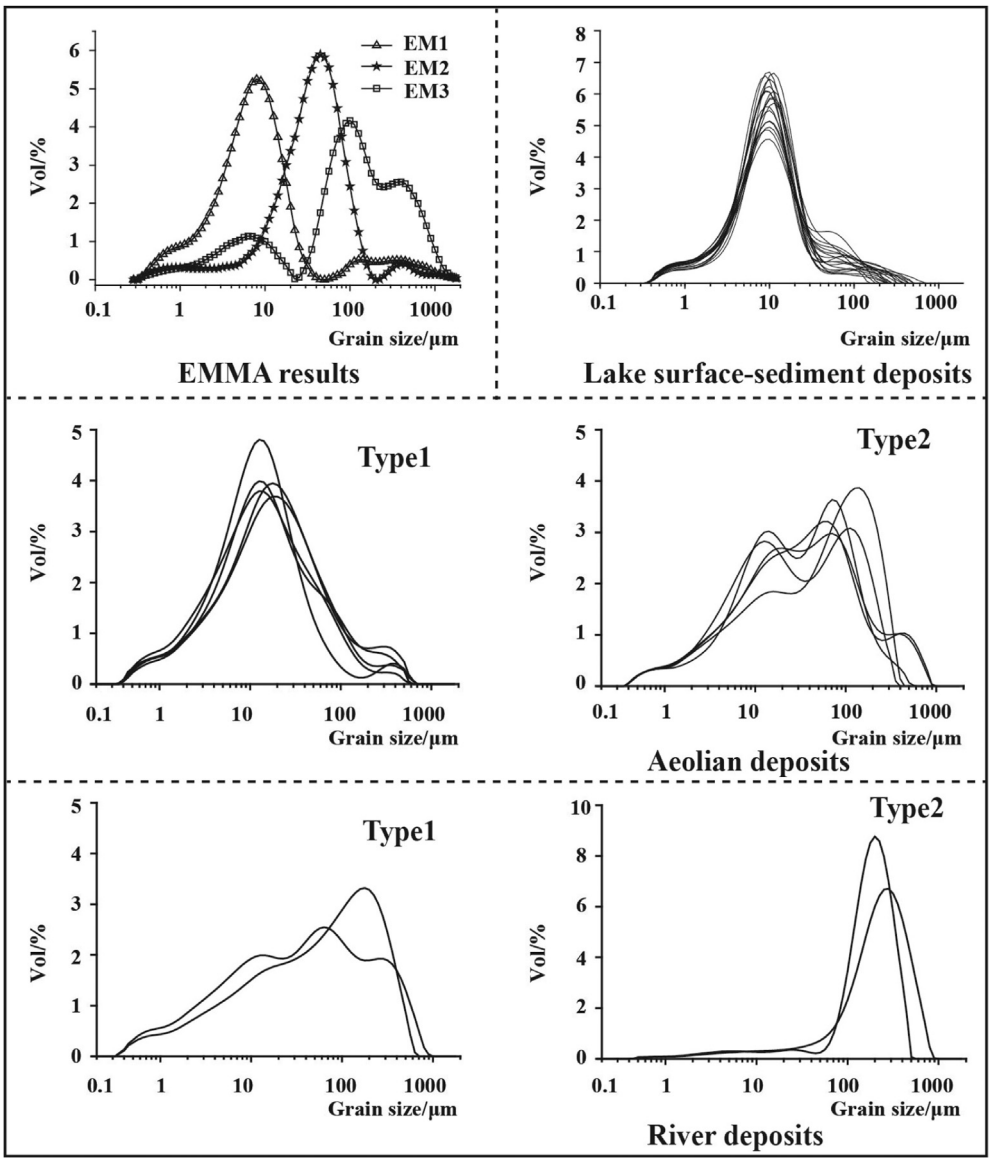

Fig. 4. Results of the optimal end-member model and individual grain-size distributions of surface samples.

4.3.2.6. Pollen zone PA (520–290 cm, 15.2–8.9 cal kyr BP). The most obvious characteristic is the increase of other pollen types (e.g., Poaceae, *Ephedra*, Cyperaceae) in addition to *Artemisia* and Amaranthaceae. The percentage of *Artemisia* pollen decreases, while *Ephedra* pollen shows an opposite trend. Wetland pollen (especially Poaceae) reaches its maximum value of 33.8% within this zone, and pollen concentrations show a major increase compared with the lower zone PB, although with clear fluctuations.

4.3.2.7. Subzone PA-3 (520–435 cm, 15.2–12.6 cal kyr BP). Meadow pollen, e.g., Poaceae (12.4%) and Cyperaceae (2.5%), increases substantially, and *Ephedra* increases to 4.6%; *Artemisia* and Amaranthaceae account for 42.0% and 29.1% on average, respectively. Poaceae pollen reaches a high level of 33.8% in the early part of this subzone but nearly vanishes at the top of this zone. Arboreal pollen, e.g., *Pinus*, *Picea*, *Betula*, and *Salix*, occurs occasionally. The pollen concentration shows a gradual increasing trend, with an average value of 11.3×10^3 grains/g.

4.3.2.8. Subzone PA-2 (435–335 cm, 12.6–10.0 cal kyr BP). *Ephedra* (13.5%) increases continuously, while Poaceae decreases to 5.0%, a sharp decrease compared with the previous subzone. *Artemisia* decreases slightly to 38.0%, while Amaranthaceae and Asteraceae account for 32.2% and 4.8% on average, respectively. The pollen concentration decreases continuously, with an average pollen concentration of 14.0×10^3 grains/g.

4.3.2.9. Subzone PA-1 (335–294 cm, 10.0–8.9 cal kyr BP). The pollen assemblages fluctuate significantly in this zone. Amaranthaceae has a high mean percentage of 44.6%, *Artemisia* decreases to 32.0% on average, and the mean value of *Ephedra* is 9.8%. Amaranthaceae reaches as high as 91.2%, while *Artemisia* accounts for only 2.9% in a sample at 315 cm (*ca.* 9.5 cal kyr BP). The pollen concentrations fluctuate from 0.3×10^3 to 10.0×10^3 grains/g.

4.3.3. Ordination analysis of the surface samples and fossil pollen

Principal components analysis shows that the first and second axes capture 38.6% and 13.3% of the total variance in the data set,

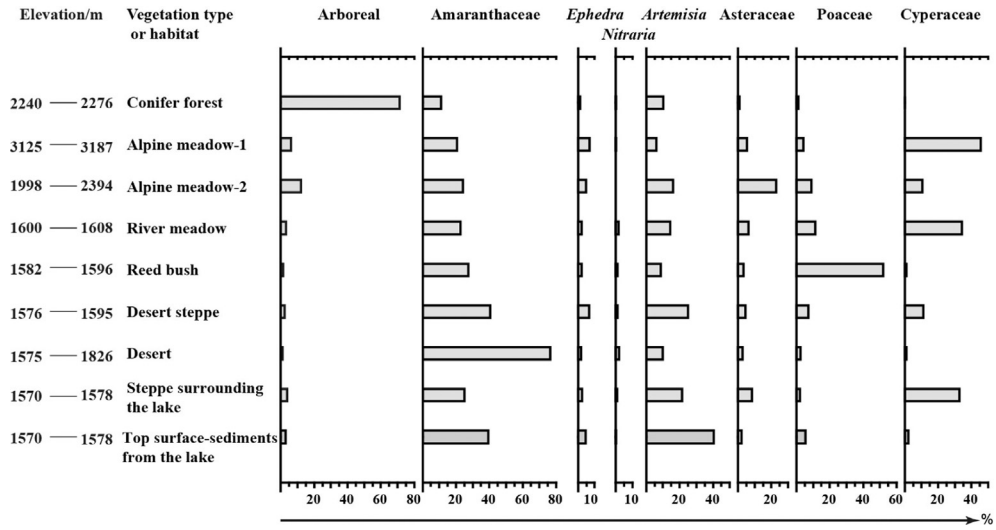

Fig. 5. Modern pollen diagram showing relative pollen abundance for the main vegetation communities in the study area. Alpine meadow-1: meadow above the conifer forest; Alpine meadow-2: meadow below the conifer forest.

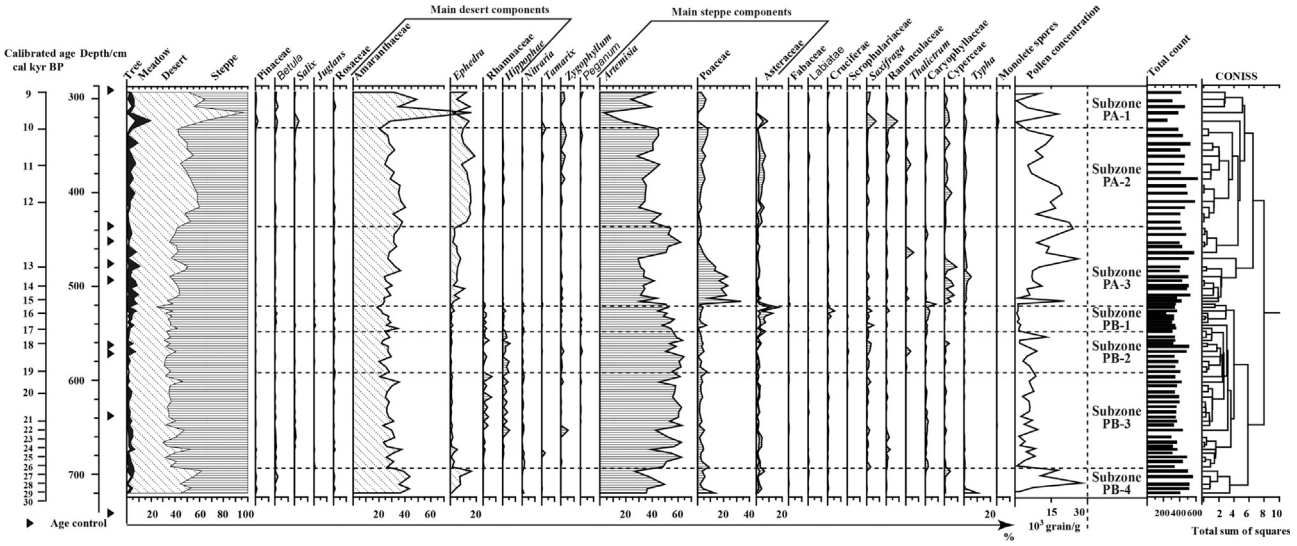

Fig. 6. Pollen diagram of the core BLK11A from Balikun Lake covering MIS2.

respectively (Fig. 7). Arboreal (e.g., *Betula*, *Salix*, Pinaceae, Ulmaceae) and warm-climate herbaceous (e.g., Poaceae, *Thalictrum*, Cyperaceae, *Typha*) pollen types have a positive trend along PCA axis 1, while hardy shrubs (e.g., *Artemisia*, Rosaceae, Rhamnaceae, *Hippophae*) have a negative trend (Fig. 7a). Therefore, axis 1 is interpreted as a temperature gradient. Samples grouped by age separate along this axis as Fig. 7b shows, and boxplots of the PCA axis 1 scores during the different periods are shown in Fig. 7c. Scores are low during the LGM, late LGM, and Heinrich event 1 (H1), while the maximum score appears in the mid-Holocene.

The major positive component of PCA axis 2 is Asteraceae, which is a family that contains mostly dwarf herbaceous plants that usually have a broad ecological amplitude and a short pollen transmission distance (Tang et al., 2012). Previous studies suggest that Asteraceae pollen conveys the most information about local soil conditions (e.g., pH, salinity, soil moisture) (Cheng and Chen, 2010): we also find it to be tightly linked with local depositional processes.

5. Discussion

5.1. Vegetation history of the Balikun region during MIS2

Pollen assemblages from core BLK11A show that *Artemisia* and Amaranthaceae are the dominant pollen species, indicating desert-steppe to desert vegetation and a persistent dry climate throughout MIS2 (Fig. 6, Table 2). The vegetation history of the Balikun region may be divided into two stages (stage I and stage II), with three substages in stage I (PA) and four substages in stage II (PB), following our pollen zones.

5.1.1. Stage II: 29.1–15.2 cal kyr BP (PB)

This stage is characterized by low pollen concentrations, indicating low vegetation cover in the Balikun basin, as well as by a high frequency of *Artemisia* pollen, suggesting a limited number of vegetation types. Previous modern pollen studies regard *Artemisia* communities as a diagnostic indicator of wetter steppe/desert

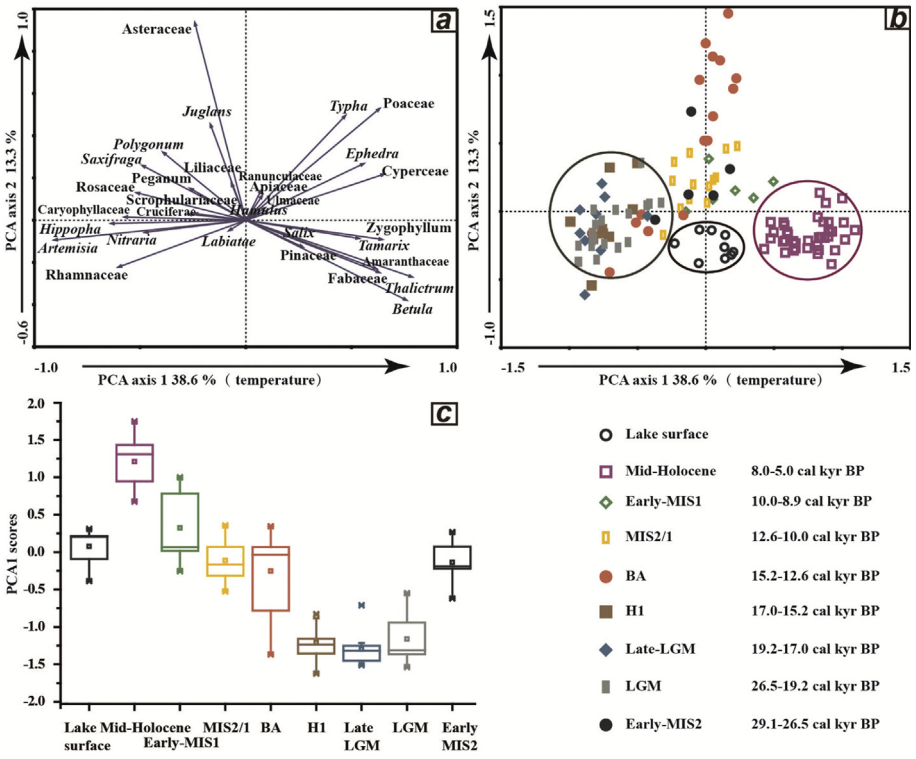

Fig. 7. Diagram showing (a, b) PCA results and (c) boxplots of PCA1 scores for modern surface samples and pollen data from core BLK11A. MIS = Marine isotope stage; BA = Bølling/Allerød; H1 = Heinrich event 1; LGM = last glacial maximum.

Table 2
Distinct biomes and typical pollen assemblages from Balikun Lake.

Pollen zone	Climatic stages	Distinct biomes	Typical pollen assemblage
(core BLK06E)	Mid-Holocene	Steppe	*Artemisia*, Amaranthaceae, *Betula*, Poaceae, Cyperaceae
PA-1	Early-MIS1	Desert	Amaranthaceae, *Artemisia*, *Ephedra*, Asteraceae,
PA-2	MIS2/1	Desert steppe	*Artemisia*, Amaranthaceae, *Ephedra*, Asteraceae, Poaceae
PA-3	BA	Steppe	*Artemisia*, Amaranthaceae, Poaceae, Cyperaceae, *Typha*
PB-1	H1	Desert	*Artemisia*, Amaranthaceae, Asteraceae, Poaceae
PB-2	Late-LGM	Desert	*Artemisia*, Amaranthaceae, Elaeagnaceae, Rhamnaceae, *Hippophae*, Zygophyllaceae, Poaceae, Saxifragaceae
PB-3	LGM	Desert	*Artemisia*, Amaranthaceae, Elaeagnaceae, Rhamnaceae, *Hippophae*, Zygophyllaceae, Poaceae
PB-4	Early-MIS2	Desert steppe	Amaranthaceae, *Artemisia*, *Ephedra*, Poaceae

MIS = Marine isotope stage; BA = Bølling/Allerød; H1 = Heinrich event 1; LGM = last glacial maximum.

steppe climate condition in arid/semi-arid areas (Coetzee, 1976; El-Moslimany, 1990) and apply this reasoning to fossil pollen data to reconstruct palaeovegetation and infer palaeoclimate. However, the interpretation of *Artemisia* fossil pollen data must consider pollen sources and depositional processes. A study by C.X. Luo et al. (2009) on modern pollen distributions and the corresponding vegetation in arid areas suggests that the ratio of relative pollen abundance of *Artemisia* to its relative plant cover in desert samples from the northern slopes of the Tienshan Mountains is as high as 15, indicating that *Artemisia* is over-represented in these pollen samples. Similar results are also reported from other study areas (Yan and Xu, 1989; Van Campo et al., 1996; Xu et al., 1996; Carrion, 2002; Yang et al., 2004). Considering the spatial heterogeneity of the water supply system in the Balikun region and the low vegetation cover during this interval, we infer that *Artemisia* communities were restricted to the eastern part of Balikun Lake, where water was locally available from the Dahe River runoff, while the desert areas expanded elsewhere as indicated by the high pollen frequency of desert shrubs such as Elaeagnaceae, Rhamnaceae, and *Hippophae*. The sparse desert plant communities produce low pollen counts, thereby allowing *Artemisia* to be over-represented in the pollen assemblage. The high frequency of *Artemisia* pollen thus represents local rather than regional vegetation. The rest of the Balikun basin was likely covered by desert or desert-steppe vegetation during this stage. Based on the variation among pollen taxa, the vegetation succession in this stage can be further divided into three sub-stages.

During the early MIS2 (29.1–26.5 cal kyr BP, PB-4), the Balikun basin was dominated by Amaranthaceae-*Artemisia*-*Ephedra*-Poaceae desert steppe; a community similar to modern vegetation (Figs. 5 and 6). The high percentages of Amaranthaceae and *Ephedra* pollen indicate a relatively dry climate. PCA shows that temperature was still relatively high, allowing small amounts of mountain glacial runoff, which could have sustained the regional development of higher vegetation cover. Afterwards an abrupt decrease in pollen occurred, with the lowest pollen concentration at approximately 26.5 cal kyr BP, indicating a deterioration of regional climate and the onset of the LGM (26.5–19.2 cal kyr BP, PB-3). Desert areas simultaneously expanded, as deduced from high frequencies of desert shrub pollen (e.g., Elaeagnaceae, Rhamnaceae, *Hippophae*,

Zygophyllaceae) and substantial declines of steppe vegetation dominated by Amaranthaceae, *Artemisia*, *Hippophae*, and Rhamnaceae. Ameliorated desert vegetation is indicated by the pollen assemblages during the late LGM (19.2–17.0 cal kyr BP, PB-2): meadow components (e.g., Poaceae, Saxifragaceae) increased a little, as did the vegetation cover, although with fluctuations. The region was still covered by *Artemisia*-Amaranthaceae-Poaceae-Saxifragaceae desert. The substage PB-1 from 17.0 to 15.2 cal kyr BP corresponds with the cold Heinrich event 1 (Heinrich, 1988; Bond et al., 1992, 1993; Hemming, 2004). Amelioration of the local vegetation was interrupted and low pollen concentrations indicate the least vegetation cover reflecting the extremely cold and dry conditions. During this interval, the Balikun basin was dominated by *Artemisia*-Amaranthaceae-Asteraceae desert.

5.1.2. Stage I: 15.2–8.9 cal kyr BP (PA)

The pollen assemblages change significantly and the vegetation types increase considerably, even though *Artemisia* and Amaranthaceae are still the main components. High pollen concentrations indicate that vegetation flourished. Stage A is divided into three substages.

Between 15.2 and 12.6 cal kyr BP (PA-3), a great increase in wetland herbs (e.g., Poaceae, Cyperaceae, *Typha*), together with the frequent appearance of arboreal pollen (e.g., *Pinus*, *Picea*, *Betula*, *Salix*), indicate rising humidity and temperature, which might be linked to the Bølling/Allerød (BA) interstadial that is clearly recorded in other regions (e.g., central Europe (Friedrich et al., 2001), Sea of Marmara (Mudie et al., 2002), Black Sea (Bahr et al., 2008)). *Artemisia* is partially replaced by Poaceae and Cyperaceae, and the region was covered by *Artemisia*-Poaceae-Amaranthaceae-Cyperaceae steppe. A notable feature during substage MIS2/1 (12.6–10.0 cal kyr BP, PA-2) is the increased proportion of *Ephedra*. *Ephedra* usually represents decreasing moisture (Sun et al., 1996; Cour et al., 1999; Herzschuh et al., 2004). Although vegetation cover was not low, the *Ephedra* community contributed much of the total pollen concentration. The Balikun region was dominated by *Artemisia*-Amaranthaceae-*Ephedra*-Asteraceae desert steppe, reflecting a sustained decrease in moisture, after which Amaranthaceae-*Artemisia*-*Ephedra* desert dominated the region during the early MIS1 (10.0–8.9 cal kyr BP, PA-1). Based on the high percentage of Amaranthaceae pollen (91.2%), Amaranthaceae must have occurred across the whole region at approximately 9.5 cal kyr BP, indicating extremely dry conditions.

5.2. Climate and its influence on regional vegetation in the Balikun region during MIS2

The impact of climate fluctuations can be observed in the dynamics of vegetation, most particularly in the sensitive environment of herbaceous-dominated grassland (Rodriguez-Iturbe et al., 1999). In our study, the alternation between distinct biomes (desert, desert-steppe, steppe) and the representative pollen types found are useful to distinguish regional temperature and moisture evolution (Table 2). Two typical cold-dry epochs (LGM, H1) and one warm-wet epoch (BA) can be identified in the Balikun region. It is well accepted that soil water availability is the controlling factor in the organization and functionality of many ecological systems in arid areas, including those related to carbon assimilation via photosynthesis control and stomatal closure, and to nitrogen assimilation through control of the nitrogen mineralization rate (Scholes and Walker, 1993). Soil moisture is dependent on a stochastic climate controlling rainfall inputs and on losses from evapotranspiration and leakage. Large-scale desert geomorphic and sedimentological evidence (Chen and Bowler, 1986; Hövermann, 1998; Yang et al., 2011) and modelling results (Li and Morrill, 2013) suggest decreasing precipitation after *ca*. 25 cal kyr BP in arid areas; generally consistent with the expansion of desert shrubs (e.g., Elaeagnaceae, Rhamnaceae, *Hippophae*, Zygophyllaceae) in the Balikun basin.

Runoff from mountain glacial meltwater is also a major contributor to soil moisture in the arid areas of the Balikun basin (Shi et al., 2007; Li et al., 2008). Local temperature variance would thus affect evaporation as well as runoff. Additionally, temperature itself is a vital factor controlling the initiation, termination, and performance of photosynthetic activity (Myneni et al., 1997). Changes in local temperature during MIS2 have been reconstructed based on PCA axis 1, which can be used as an indication of climate evolution processes.

Temperature during the LGM, late LGM, and H1 was lower than in the other periods (Figs. 7 and 8). From the LGM to H1, the sustained low temperatures along with dry climate conditions not only had strong negative impacts on vegetation but also changed hydrological conditions and runoff substantially. Water was locked up by growing mountain glaciers during the LGM, lowering the lake level, expanding the desert region, and reducing the vegetation cover substantially. Published palaeodata show that periglacial landforms prevailed during the LGM in the surrounding regions of the Gobi Desert due to the much lower than present mean annual temperature (e.g., Hexi Corridor (Wang et al., 2003); Taklamakan Desert (Yang et al., 2006)). In the late LGM, climate ameliorated, but temperature was still low. An extremely cold and dry climate prevailed from 17.0 to 15.2 cal kyr BP, a time interval corresponding to the cold Heinrich event 1 (H1, Bond et al., 1992, 1993; Heinrich, 1988; Hemming, 2004); the desert expanded again and vegetation had its lowest cover, indicating limited regional biomes.

Temperature changes represented by PCA axis 1 suggest that the temperature in early MIS2, BA, and MIS2/1 was close to modern conditions, but climate was warmer than that of today during the middle Holocene (Figs. 7c and 8). The relatively high vegetation cover is inferred as a response to the milder climate. The marked increase in Poaceae during the BA period indicates that the climate was relatively warm and that water supplied from mountain glacial runoff played an important role in the local vegetation boom. Subsequently, temperatures rose persistently in the Balikun basin.

Tao et al. (2010) document climate changes in the mid-Holocene (*ca*. 8–5 cal kyr BP) based on pollen data and grain-size frequency of core BLK06E in our investigated area. However, our results from core BLK11A show significant discrepancies regarding changes in insolation and glacial boundary conditions (ice volume) in the mid-Holocene as well as during MIS2. Although the region was still mainly covered by *Artemisia* and Amaranthaceae during the mid-Holocene, the relative pollen abundance of Poaceae indicates that the steppe area expanded. Such warm and wet climate conditions favour the development of arboreal vegetation (especially *Betula*) and high vegetation cover. We find that vegetation dynamics in the Balikun region are tightly linked to temperature modulated by July insolation (Fig. 8): desert vegetation with low vegetation cover prevailed during cold periods, and the decrease of precipitation together with the inferred shortage of mountain glacial runoff expected under the low temperature with lower insolation regime, contributed to the reduced soil moisture and degraded vegetation. In contrast, steppe vegetation is associated with warm conditions with higher insolation. In response to the changed local temperature and moisture conditions triggered by variation in summer insolation, the vegetation in our study area underwent significant ecological evolution.

5.3. Evolution of Balikun Lake during MIS2 and comparisons with regional palaeoclimate records

The EMMA results have been used to evaluate sedimentation

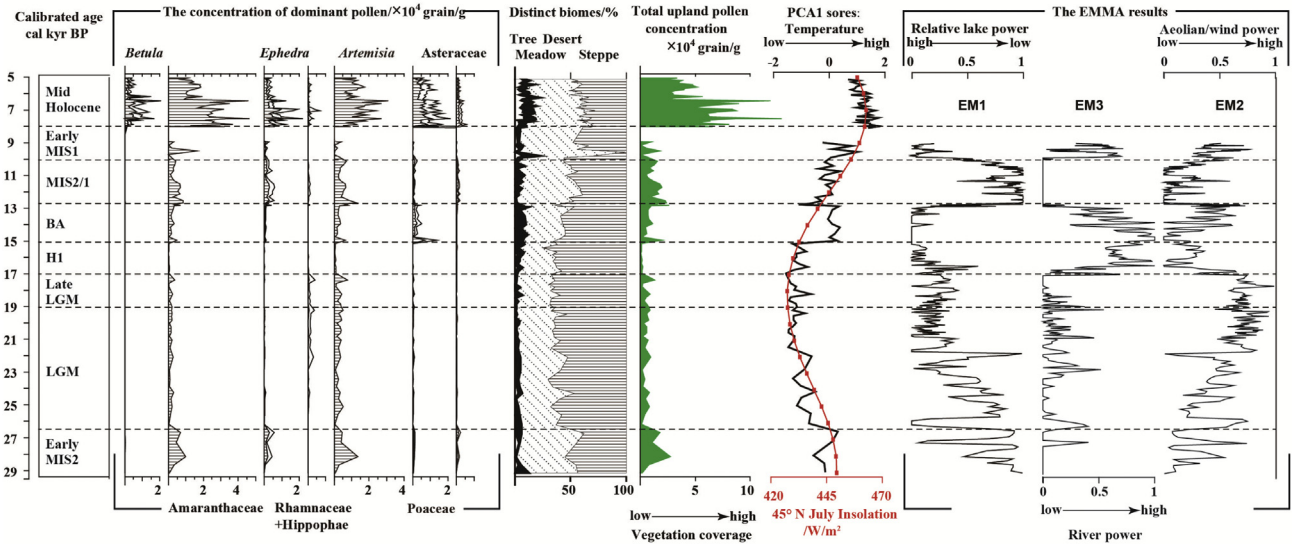

Fig. 8. Diagram showing pollen concentration changes for typical pollen taxa, the end-member modelling analysis (EMMA) results of core BLK11A, and the change in July insolation at 45°N (Laskar et al., 2004). The data for the mid-Holocene (*ca.* 8–*ca.* 5 cal kyr BP) are from core BLK06E (Tao et al., 2010).

environments and processes (e.g., Dietze et al., 2012, 2013). Our EMMA results agree well with the pollen zones (Fig. 8). As Balikun Lake has a flat bottom, a small change in lake level would have a large effect on lake area, affecting the sedimentary and sorting processes.

5.3.1. Early MIS2 (29.1–26.5 cal kyr BP, PB-4)

The high content of unimodal sequence EM 1 suggests a weak lacustrine circulation under calm water conditions, similar to the present-day condition. More fine material was deposited during the warm and wet MIS3 (Zhang and Wünnemann, 1997; Zhang et al., 2001, 2002, 2004), and the gradually decreasing loading of EM 1 and increasing loading of EM 2 indicate that climate was probably in a transition from warm, wet MIS3 to cold, dry MIS2. At Luanhaizi, *ca.* 1000 km to the south-east, a shallow lake with oligohaline to mesohaline conditions appeared and the decreasing productivity of its submerged vegetation is inferred to indicate a deteriorating climate (Herzschuh et al., 2005). At Lake Baikal, sedimentary organic matter declined across this transitioning phase corresponded to the glacial conditions (Swann et al., 2005). PCA axis 1 demonstrates that local temperatures remained high until the LGM and that the lake level was similar to the present-day level.

5.3.2. LGM (26.5–19.2 cal kyr BP, PB-3)

Balikun Lake existed as a very shallow lake during and after the LGM, until 15.2 cal kyr BP, and the high loading of EM 2 indicates that aeolian deposits increased during this time. Similarly, deserts in most parts of arid China expanded significantly during the LGM, indicating cold and dry climate conditions (Sun et al., 1998; Dong, 2002; Lancaster et al., 2013; Lu et al., 2013; Yang et al., 2013; Chen et al., 2014; Williams, 2014).

In arid western China, however, the interpretations of lacustrine records during the LGM are still hotly debated. Yu et al. (2003) synthesized lake records in China and concluded that most of the lakes in western China have experienced a higher LGM lake level compared to that of the present, but Li and Morrill (2013) found discrepancies due to the shortage of well-dated records synthesized by Yu et al. (2003). Moreover, previous modelling studies considered only precipitation and evapotranspiration changes as causes of lake-level fluctuations (Qin and Yu, 1998; Yu et al., 2003), regardless of lake-surface evaporation and changes in runoff, which also play a significant role in lake-water balance (Li and Morrill, 2010).

Many lakes in arid western China were mainly supplied by meltwater from snow and glaciers in the surrounding mountains. Some studies show that the LGM annual temperature was *ca.* 10 °C lower than the present in arid western China (e.g., Hövermann and Hövermann, 1991; Yang, 1991; Yang et al., 2002; Liu et al., 2002) in response to decreases in the high-latitude summer insolation and other boundary conditions (Clark et al., 2009). The existence of mountain glaciers (Grosswald et al., 1994; Narama et al., 2007; Takeuchi et al., 2014) and their limited meltwater contributions, may have resulted in a contemporaneous lake lowstand. Recently, comparable lowstands have been reported from many lakes in western China (e.g., Manas Lake (Rhodes et al., 1996); Hala Lake (Yan and Wünnemann, 2014); Aydin Lake (Li et al., 1989); Lop Nur (Yan et al., 1998); Balikun Lake (An et al., 2013); Luanhaizi (Herzschuh et al., 2005); Baijian Lake (Pachur et al., 1995; Zhang et al., 2004)).

The general pattern of widespread aridity during the LGM is generally supported by multidisciplinary data such as pollen and other proxies. Low organic carbon and carbonate contents and the lack of aquatic vegetation remains in lake sediments point to a desiccation or freezing of the lake for most of the year (Herzschuh et al., 2005). Zhao et al. (2013) report that, in the Yili valley, the forest steppe dominated by *Picea* and *Taraxacum* was replaced by Chenopodiaceae during this cold interval. Sparse alpine vegetation and alpine deserts occurred in the vicinity of Luanhaizi, indicating dry conditions in the Qilian Mountains (Herzschuh et al., 2006). Other studies from arid central Asia also demonstrate an analogously dry condition: very low water levels are reported for Hovsgol Lake in Mongolia during the LGM (Prokopenko et al., 2005), and at both Baikal and Hovsgol Lakes, planktonic and benthic diatoms are absent in the sedimentary record (Karabanov et al., 2004).

5.3.3. The late LGM and H1 (19.2–15.0 cal kyr BP, PB-2)

Clark et al. (2009) assume that the end of the LGM largely depended on the increase in northern summer insolation: the earlier retreat of Northern Hemispheric mountain glaciers was

synchronous within error at *ca*. 19 cal kyr BP. The increased runoff produced by the rising temperature would first benefit the vegetation; ameliorating the desert vegetation as revealed by our pollen assemblages from Balikun Lake. Previous studies suggest that an increase in insolation could also trigger higher moisture levels initially and thus glacial accumulation, leading to prolonged cold and dry climatic conditions and helping buffer against the onset of warmer conditions (Cook et al., 2011). As a result, the lacustrine circulation would not change substantially. The period from 17 to 15 cal kyr BP is roughly correlated to the well-known Heinrich event 1 (H1), characterized by a decrease in sea-surface temperature and salinity in the North Atlantic allowing abundant ice and ice-rafted debris to be exported into the ocean (Heinrich, 1988; Bond et al., 1992, 1993; Hemming, 2004). The water body of Balikun Lake was restricted to the centre of the basin, the distance from the river mouth to the lake centre was sharply shortened, allowing more poorly-sorted littoral and near-shore materials with a multimodal size distribution (EMs 2 and 3) to be deposited in the lake, and the least vegetation cover permitted the largest amount of aeolian deposits to enter the lake. The climate is therefore interpreted as cold and dry, with the lake area shrunken to its minimum during MIS2.

5.3.4. BA to early MIS1 (15.0–8.9 cal kyr BP, PA)

The increase in the loading of EM 3 (typical river deposits) represents strong runoff in the early part of the BA interstadial. Our PCA axis 1 suggests a higher local temperature, and together with a high percentage of wetland herbs (e.g., Poaceae, Cyperaceae, *Typha*), indicates a warm and wet climate. This deglaciation event in the Tienshan Mountains has also been noted by previous investigators (Osmonov, 1991; Thompson et al., 1997; Romanovskiy, 2007). Takeuchi et al. (2014) find that the BA is likely to be the glacial minimum in the period from the LGM to the present in the Tien Shan region. In the late phase of the BA interstadial, lake level began to rise as inferred from the increase of the loading of EM 1; the increasing supply of meltwater extended the distance from the river mouth to the centre of the lake, which in turn weakened the influence of river flow. Evidence of this climate event can also be found in other areas of arid central Asia: rising water levels occurred at *ca*. 15.4 cal kyr BP in Hovsgol Lake (Prokopenko et al., 2005) and Hala Lake (Yan and Wünnemann, 2014).

During the following MIS2/1 interval, the lacustrine circulation weakened and the lake level was stable, as revealed by the high loading of EM 1. A gradually rising temperature, on the one hand, may have brought more runoff to Balikun basin, and on the other hand, increased the rate of evaporation. The dynamic interactions between them balanced the water budget and determined the evolutionary direction of the lake. The influence of meltwater from glaciers was weakened due to the loss of glacial area and volume, increasing the importance of local rainfall. Our pollen results suggest a warm and dry climate in the Balikun region. Although the Younger Dryas (YD) event is not clearly recorded in the Balikun core, the EMMA results do show some changes at *ca*. 11.5 cal kyr BP, with a slightly higher loading of EM 2 and low pollen concentrations. Dykoski et al. (2005) suggest that only the largest deglaciation events trigger an observable response in China because of the influence of snow cover on the Tibetan Plateau, which effectively buffers against the impact of lower-magnitude events.

A prominent decrease in lake level with apparent fluctuations likely occurred during early MIS1. An increased loading of EM 2 and EM 3 indicates that the lacustrine circulation became strong, and when the lake level dropped, dynamic fluvial activity might have eroded the previous lake shore and delivered more coarse sediments to the lake. The expansion of the desert area revealed by pollen assemblages suggests an enhanced drought condition. Our results are consistent with published studies in western China and arid central Asia, for example, Bosten Lake (Huang et al., 2009), Wulungu Lake (Jiang et al., 2007), Gun Nuur (Wang et al., 2004; Feng et al., 2005), the Aral Sea (Boomer et al., 2000), and the Caspian Sea (Kazanci et al., 2004).

6. Conclusions

A high-resolution lacustrine record of vegetation history and climate conditions during MIS2 has been reconstructed based on pollen and grain-size data from a sediment core (BLK11A) in Balikun Lake in arid western China. The vegetation in the Balikun basin during MIS2 showed an alternating pattern from desert steppe (early-MIS2), to desert (LGM, late-LGM, H 1), to steppe (BA), to desert steppe (MIS2/1), and to desert (early-MIS1). During most periods of MIS2, *Artemisia* and Amaranthaceae were the key components of the vegetation community. The vegetation cover was low, and Balikun Lake was relatively shallow experiencing high aeolian deposition, suggesting persistently dry climate conditions in our study region during MIS2.

Extremely cold and dry conditions prevailed between 17.0 and 15.2 cal kyr BP, an interval corresponding to Heinrich event 1. The Balikun region had the least vegetation cover, and Balikun Lake shrank to its minimum level during MIS2. There was an exceptional period (15.2–12.6 cal kyr BP) of relatively warm and wet conditions during the BA (Bølling/Allerød) interstadial, which was characterized by high vegetation cover and *Artemisia*-Amaranthaceae-Poaceae steppe, and lake level began to rise due to increased runoff.

The landscape development was tightly associated with the spatial heterogeneity of water supply system: mountain glacial runoff from the east parts of the Balikun basin caused the high pollen percentage of *Artemisia* during the LGM (26.5–19.2 cal kyr BP), while the desert areas simultaneously expanded, as indicated by the high pollen frequency of desert shrubs (e.g., Elaeagnaceae, Rhamnaceae, *Hippophae*) and low vegetation cover. This cold and dry LGM climate triggered an extensive lowering of lake level in most of arid western China.

Changes in local temperature and moisture regulated by the variations in local July insolation are inferred to have exerted a remarkable influence on the evolution of vegetation communities and lake level in our study area.

Acknowledgements

This study is supported by the National Natural Science Foundation of China (NSFC, Grants 41130102, 41372170). Our sincere thanks are extended to two anonymous reviewers and the Editor, Prof. Xiaoping Yang, for very helpful comments and constructive suggestions that greatly improved this manuscript. We also would like to thank Drs. Shi-Yong Yu and Cathy Jenks for polishing the language and improving the scientific significance of this paper.

References

An, C.B., Lv, Y.B., Zhao, J.J., Tao, S.C., Dong, W.M., Li, H., Jin, M., Wang, Z.L., 2012a. A high resolution record of Holocene environmental and climatic changes from Lake Balikun (Xinjiang): implications for Central Asia. Holocene 22, 43–52.

An, C.B., Tao, S.C., Zhao, J.J., Chen, F.H., Lv, Y.B., Dong, W.M., Zhao, Y.T., Wang, Z.L., 2013. Late Quaternary (30.7–9.0 cal ka BP) vegetation history in Central Asia inferred from pollen records of Lake Balikun, northwest China. J. Paleolimnol. 49 (2), 145–154.

An, Z.S., Colman, S.M., Zhou, W., Li, X., Brown, E.T., Timothy Jull, A.J., Cai, Y., Huang, Y., Lu, X., Chang, H., Song, Y., Sun, Y., Xu, H., Liu, W., Jin, Z., Liu, X., Cheng, P., Liu, Y., Ai, L., Li, X., Yan, L., Shi, Z., Wang, X., Wu, F., Qiang, X., Dong, J., Lu, F., Xu, X., 2012b. Interplay between the Westerlies and Asian monsoon recorded in Lake Qinghai sediments since 32.5 ka. Sci. Rep. 2, 619.

Bahr, A., Lamy, F., Arz, H.W., Major, C., Kwiecien, O., Wefer, G., 2008. Abrupt changes of temperature and water chemistry in the late Pleistocene and early Holocene

Black Sea. Geochem. Geophys. Geosyst. 9 (1), 1–16.
Bigelow, N.H., Brubaker, L.B., Edwards, M.E., Harrison, S.P., Prentice, I.C., Anderson, P.M., Andreev, A.A., Bartlein, P.J., Christensen, T.R., Cramer, W., Kaplan, J.O., Lozhkin, A.V., Matveyeva, N.V., Murray, D.F., McGuire, A.D., Razzhivin, V.Y., Ritchie, J.C., Smith, B., Walker, D.A., Gajewski, K., Wolf, V., Holmqvist, B.H., Igarashi, Y., Kremenetskii, K., Paus, A., Pisaric, M.F.J., Volkova, V.S., 2003. Climate change and Arctic ecosystems: 1. Vegetation changes north of 55°N between the last glacial maximum, mid-Holocene, and present. J. Geophys. Res. 108 (D19), 8170.
Bond, G., Heinrich, H., Huon, H., Broecker, L., Labeyrie, J., Audrews, J., Mcmanus, S., Clasen, K., Tedesco, R., Jantschink, C., Simet, Mieczyslawa, K., 1992. Evidence for massive discharges of icebergs into the glacial Northern Atlantic. Nature 360, 245–249.
Bond, G., Broecker, W., Johnsen, S., McManus, J., Labeyrie, L., Jouzel, J., Bonani, G., 1993. Correlations between climate records from North Atlantic sediments and Greenland ice. Nature 365 (6442), 143–147.
Boomer, Aladin, N.V., Plotnikov, I.S., Whatley, R., 2000. The palaeolimnology of the Aral Sea: a review. Quat. Sci. Rev. 19, 1259–1278.
Carrion, J.S., 2002. A taphonomic study of modern pollen assemblages from dung and surface sediments in arid environments of Spain. Rev. Palaeobot. Palynol. 120, 217–232.
Chen, F.H., Li, G.Q., Zhao, H., Jin, M., Chen, X.M., Fan, Y.X., Liu, X.K., Madsen, D., 2014. Landscape evolution of the Ulan Buh Desert in northern China during the late Quaternary. Quat. Res. 81 (3), 476–487.
Chen, K., Bowler, J.M., 1986. Late Pleistocene evolution of salt lakes in the Qaidam basin, Qinghai province, China. Palaeogeogr. Palaeoclimatol. Palaeoecol. 54, 87–104.
Cheng, B., Chen, F.H., 2010. Pollen analysis of topsoil samples from Shiyang River drainage, Northwest China. J. Desert Res. 30, 350–356 (in Chinese).
Clark, P.U., Dyke, A.S., Shakun, J.D., Carlson, A.E., Clark, J., Wohlfarth, B., Mitrovica, J.X., Hostetler, S.W., McCabe, A.M., 2009. The last glacial maximum. Science 325 (5941), 710–714.
Coetzee, J.A., 1976. Pollen analytical studies in east and southern Africa. Palaeoecol. Afr. 3, 1–146.
Cook, C.G., Jones, R.T., Langdon, P.G., Leng, M.J., Zhang, E., 2011. New insights on Late Quaternary Asian palaeomonsoon variability and the timing of the Last Glacial maximum in southwestern China. Quat. Sci. Rev. 30 (7), 808–820.
Cour, P., Zheng, Z., Duzer, D., Calleja, M., Yao, Z., 1999. Vegetation and climatic significance of modern pollen rain in northwestern Tibet. Rev. Palaeobot. Palynol. 104, 183–204.
Dietze, E., Hartmann, K., Diekmann, B., IJmker, J., Lehmkuhl, F., Opitz, S., Stauch, G., Wünnemann, B., Borchers, A., 2012. An end-member algorithm for deciphering modern detrital processes from lake sediments of Lake Donggi Cona, NE Tibetan Plateau, China. Sediment. Geol. 243–244, 169–180.
Dietze, E., Wünnemann, B., Hartmann, K., Diekmann, B., Jin, H., Stauch, G., Yang, S., Lehmkuhl, F., 2013. Early to mid-Holocene lake high-stand sediments at Lake Donggi Cona, northeastern Tibetan Plateau, China. Quat. Res. 79 (3), 325–336.
Dong, G.R., 2002. Studies on Deserts Formation and Evolution, Climate Changes and Desertification in China. China Ocean Press, Beijing, p. 734 (in Chinese).
Dykoski, C.A., Edwards, R.L., Cheng, H., Yuan, D., Cai, Y., Zhang, M., Lin, Y.S., Qing, J.M., An, Z.S., Revenaugh, J., 2005. A high-resolution, absolute-dated Holocene and deglacial Asian monsoon record from Dongge Cave, China. Earth Planet. Sci. Lett. 233 (1), 71–86.
El-Moslimany, A.P., 1990. The ecological significance of common nonarboreal pollen: examples from drylands of the Middle East. Rev. Palaeobot. Palynol. 64, 343–350.
Fægri, K., Iversen, J., 1989. Textbook of Pollen Analysis, fourth ed. John Wiley and Sons, London, UK.
Feng, Z.D., Wang, W.G., Guo, L.L., Khosbayar, P., Narantsetseg, T., Jull, A.J.T., An, C.B., Li, X.Q., Zhang, H.C., Ma, Y.Z., 2005. Lacustrine and eolian records of Holocene climate changes in the Mongolian Plateau: preliminary results. Quat. Int. 136, 25–32.
Friedrich, M., Kromer, B., Kaiser, K.F., Spurk, M., Hughen, K.A., Johnsen, S.J., 2001. High-resolution climate signals in the Bolling-Allerod Interstadial (Greenland Interstadial 1) as reflected in European tree-ring chronologies compared to marine varves and ice-core records. Quat. Sci. Rev. 20 (11), 1223–1232.
Grimm, E.C., 1987. CONISS: a FORTRAN 77 program for stratigraphically constrained cluster analysis by the method of incremental sum of squares. Comput. Geosci. 13 (1), 13–35.
Grimm, E.C., 2004. TILIA and TILIA.GRAPH v.2.0.2. Illinois State Museum, Springfield, USA.
Grosswald, M.G., Kuhle, K., Fastook, J.L., 1994. Würm glaciation of Lake Issyk-Kul area, Tian Shan Mts. A case study in glacial history of Central Asia. Geojournal 33, 273–310.
Han, S.T., Pan, A.D., Zhao, Q.H., 1989. Bio-stratigraphy and palaeoclimate during late Quaternary in Barkol Lake, Xinjiang. Chin. Sci. Bull. 15, 1168–1172.
Heinrich, H., 1988. Origin and consequences of cyclic ice rafting in the northeast Atlantic Ocean during the past 130,000 years. Quat. Res. 29 (2), 142–152.
Hemming, S.R., 2004. Heinrich events: massive late Pleistocene detritus layers of the North Atlantic and their global climate imprint. Rev. Geophys. 42 (1), 1–43.
Herzschuh, U., 2006. Palaeo-moisture evolution in monsoonal Central Asia during the last 50,000 years. Quat. Sci. Rev. 25 (1), 163–178.
Herzschuh, U., Tarasov, P., Wünnemann, B., Hartmann, K., 2004. Holocene vegetation and climate of the Alashan Plateau, NW China, reconstructed from pollen data. Palaeogeogr. Palaeoclimatol. Palaeoecol. 211 (1–2), 0031–0182.
Herzschuh, U., Zhang, C., Mischke, S., Herzschuh, R., Mohammadi, F., Mingram, B., Kurschner, H., Piedel, F., 2005. A late Quaternary lake record from the Qilian Mountains (NW China), evolution of the primary production and the water depth reconstructed from macrofossil, pollen, biomarker and isotope data. Glob. Planet. Change 46 (1–4), 361–379.
Herzschuh, U., Kurschner, H., Mischke, S., 2006. Temperature variability and vertical vegetation belt shifts during the last 50,000 yr in the Qilian Mountains (NE margin of the Tibetan Plateau, China). Quat. Res. 66, 133–146.
Hövermann, J., 1998. Zur Paläoklimatologie Zentralasiensequantitative Bestimmung von Paläoniederschlag und -temperature. Petermanns Geogr. Mittl. 142, 251–257 (in German).
Hövermann, J., Hövermann, E., 1991. Pleistocene and Holocene geomorphological features between the Kunlun Mountains and the Taklimakan Desert. Die Erde Erg.-H 6, 51–72.
Huang, X.Z., Chen, F.H., Fan, Y.X., Yang, M.L., 2009. Dry late-glacial and early Holocene climate in arid central Asia indicated by lithological and palynological evidence from Bosten Lake, China. Quat. Int. 194 (1), 19–27.
Integrative Investigate Team of Xinjiang and Plant Institute of Chinese Academy of Sciences, 1978. Xinjiang Vegetation and Land-use. Science Press, Beijing, pp. 251–252 (in Chinese).
Jiang, Q.F., Shen, J., Liu, X.Q., Zhang, E.L., Xiao, X.Y., 2007. A high resolution climatic change since Holocene inferred from multi-proxy of lake sediment in westerly area of China. Chin. Sci. Bull. 52, 1970–1979.
Ju, L.X., Wang, H.J., Jiang, D.B., 2007. Simulation of the Last Glacial Maximum climate over East Asia with a regional climate model nested in a general circulation model. Palaeogeogr. Palaeoclimatol. Palaeoecol. 248 (3), 376–390.
Karabanov, E., Williams, D., Kuzmin, M., Sideleva, V., Khursevich, G., Prokopenko, A., Solotchina, E., Tkachenko, L., Fedenya, S., Kerber, E., 2004. Ecological collapse of Lake Baikal and Lake Hovsgol ecosystems during the Last Glacial and consequences for aquatic species diversity. Palaeogeogr. Palaeoclimatol. Palaeoecol. 209, 227–243.
Kazanci, N., Gulbabazadeh, T., Leroy, S.A.G., Ileri, O., 2004. Sedimentary and environmental characteristics of the Gilan-Mazenderan plain, northern Iran: influence of long- and short-term Caspian water level fluctuations on geomorphology. J. Mar. Syst. 46, 145–168.
Kislov, A.V., Toropov, P.A., 2011. Modeling extreme Black Sea and Caspian Sea levels of the past 21,000 years with general circulation models. In: Buynevich, I.V., Yanko-Hombach, V., Gilbert, A.S., Martin, R.E. (Eds.), Geology and Geoarchaeology of the Black Sea Region: Beyond the Flood Hypothesis, Geological Society of America, Special Paper 473, pp. 27–32.
Kislov, A.V., Panin, A., Toropov, P.A., 2012. Palaeostages of the Caspian Sea as a set of regional benchmark tests for the evaluation of climate model simulations. Clim. Past. Discuss. 8 (5), 5053–5081.
Kislov, A.V., Panin, A., Toropov, P.A., 2014. Current status and palaeostages of the Caspian Sea as a potential evaluation tool for climate model simulations. Quat. Int. 345, 48–55.
Kostrova, S.S., Meyer, H., Chapligin, B., Tarasov, P.E., Bezrukova, E.V., 2014. The last glacial maximum and late glacial environmental and climate dynamics in the Baikal region inferred from an oxygen isotope record of lacustrine diatom silica. Quat. Int. 348, 25–36.
Lancaster, N., Yang, X., Thomas, D., 2013. Spatial and temporal complexity in Quaternary desert datasets: implications for interpreting past dryland dynamics and understanding potential future changes. Quat. Sci. Rev. 78, 301–302.
Laskar, J., Robutel, P., Joutel, F., Gastineau, M., Correia, A.C.M., Levrard, B., 2004. A long-term numerical solution for the insolation quantities of the Earth. Astron. Astrophys. 428 (1), 261–285.
Li, B.X., Cai, B.Q., Liang, Q.S., 1989. The sedimentary characteristics of aydin Lake, Turpan Basin, xinjiang, China. Chin. Sci. Bull. 34 (8), 608–610.
Li, C.X., Song, Y.G., Qian, L.B., Wang, L.M., 2011. The history of climate change recorded by the grain size at the Zhaosu loess section in central Asia since the last glacial period. Acta Sedimentol. Sin. 29 (6), 1170–1179 (in Chinese).
Li, J.J., 1990. The patterns of environmental changes since the late Pleistocene in northwestern China. Quat. Res. 3, 197–204 (in Chinese).
Li, X., Cheng, G., Jin, H., Kang, E., Che, T., Jin, R., Wu, L., Nan, Z., Wang, J., Shen, Y., 2008. Cryospheric change in China. Glob. Planet. Change 62, 210–218.
Li, Y., Morrill, C., 2010. Multiple factors causing Holocene lake-level change in monsoonal and arid central Asia as identified by model experiments. Clim. Dyn. 35, 1119–1132.
Li, Y., Morrill, C., 2013. Lake levels in Asia at the Last Glacial maximum as indicators of hydrologic sensitivity to greenhouse gas concentrations. Quat. Sci. Rev. 60, 1–12.
Lisiecki, L.E., Raymo, M.E., 2005. A Pliocene-Pleistocene stack of 57 globally distributed benthic $\delta^{18}O$ records. Paleoceanography 20, PA1003.
Liu, T., Zhang, X., Xiong, S., Qin, X., Yang, X., 2002. Glacial environments on the Tibetan Plateau and global cooling. Quat. Int. 97–98, 133–139.
Lu, H., Yi, S., Xu, Z., Zhou, Y., Zeng, L., Zhu, F., Feng, H., Dong, L., Zhuo, H., Yu, K., Mason, J., Wang, X., Chen, Y., Lu, Q., Wu, B., Dong, Z., Qu, J., Wang, X., Guo, Z., 2013. Chinese deserts and sand fields in Last Glacial Maximum and Holocene Optimum. Chin. Sci. Bull. 58 (23), 2775–2783.
Luo, C., Peng, Z.C., Yang, D., Liu, W.G., Zhang, Z.F., He, J.F., Chou, C.L., 2009a. A lacustrine record from Lop Nur, Xinjiang, China: implications for paleoclimate change during Late Pleistocene. J. Asian Earth Sci. 34 (1), 38–45.
Luo, C.X., Zheng, Z., Tarasov, P., Pan, A., Huang, K., Beaudouin, C., An, F., 2009b. Characteristics of the modern pollen distribution and their relationship to vegetation in the Xinjiang region, northwestern China. Rev. Paleobot. Palynol.

153 (3), 282–295.
Ma, Z., Wang, Z., Liu, J., Yuan, B., Xiao, J., Zhang, G., 2004. U-series chronology of sediments associated with Late Quaternary fluctuations, Balikun Lake, northwestern China. Quat. Int. 121 (1), 89–98.
Mamedov, E.D., 1991. Paleo climatic models. In: Sevastyanov, D.V. (Ed.), History of Lake Sevan, Issyk-kul, Balkhash, Zaisan and Aral. Leningrad, pp. 225–226 (in Russian).
Markova, A.K., Simakova, A.N., Puzachenko, A.Y., 2009. Ecosystems of Eastern Europe at the time of maximum cooling of the Valdai glaciation (24–18 kyr BP) inferred from data on plant communities and mammal assemblages. Quat. Int. 201, 53–59.
Mischke, S., Herzschuh, U., Zhang, C., Bloemendal, J., Riedel, F., 2005. A Late Quaternary lake record from the Qilian Mountains (NW China): lake level and salinity changes inferred from sediment properties and ostracod assemblages. Glob. Planet. Change 46 (1), 337–359.
Mithen, S., 2006. After the Ice: a Global Human History, 20,000–5,000 BC. Harvard University Press, p. 670.
Mix, A.C., Bard, E., Schneider, R., 2001. Environmental processes of the ice age: land, oceans, glaciers (EPILOG). Quat. Sci. Rev. 20, 627–657.
Mudie, P.J., Rochon, A., Aksu, A.E., 2002. Pollen stratigraphy of Late Quaternary cores from Marmara Sea: land-sea correlation and paleoclimatic history. Mar. Geol. 190, 233–260.
Müller, S., Tarasov, P.E., Hoelzmann, P., Bezrukova, E.V., Kossler, A., Krivonogov, S.K., 2014. Stable vegetation and environmental conditions during the last glacial maximum: new results from Lake kotokel (Lake baikal region, southern Siberia, Russia). Quat. Int. 348, 14–24.
Myneni, R.B., Keeling, C.D., Tucker, C.J., Asrar, G., Nemani, R.R., 1997. Increased plant growth in the northern high latitudes from 1981 to 1991. Nature 386 (6626), 698–702.
Nara, F.W., Watanabe, T., Kakegawa, T., Minoura, K., Imai, A., Fagel, N., Horiuchi, K., Nakamura, T., Kawai, T., 2014. Biological nitrate utilization in south Siberian lakes (Baikal and Hovsgol) during the Last Glacial period: the influence of climate change on primary productivity. Quat. Sci. Rev. 90, 69–79.
Narama, C., Kondo, R., Tsukamoto, S., Kajiura, T., Ormukov, C., Abdrakhmatov, K., 2007. OSL dating of glacial deposits during the Last Glacial in the Terskey-Alatoo Range, Kyrgyz Republic. Quat. Geochronol. 2 (1), 249–254.
Osmonov, A.O., 1991. The Central tien shan glacier resources. Tr. TFGC, Izd. Ilim. 40–64 (in Russian).
Pachur, H.J., Wünnemann, B., Zhang, H.C., 1995. Lake evolution in the Tengger Desert, Northwestern China, during the last 40,000 years. Quat. Res. 44 (2), 171–180.
Peng, Y., Xiao, J., Nakamura, T., Liu, B., Inouchi, Y., 2005. Holocene East Asian monsoonal precipitation pattern revealed by grain-size distribution of core sediments of Daihai Lake in Inner Mongolia of north-central, China. Earth Planet. Sci. Lett. 3, 467–479.
Prokopenko, A.A., Kuzmin, M.I., Williams, D.F., Gelety, V.F., Kalmychkov, G.V., Gvozdkov, A.N., Solotchin, P.A., 2005. Basin-wide sedimentation changes and deglacial lake-level rise in the Hovsgol basin, NW Mongolia. Quat. Int. 136, 59–69.
Qin, B., Yu, G., 1998. Implications of lake level variations at 6 ka and 18 ka in mainland Asia. Glob. Planet. Change 18 (1), 59–72.
Reimer, P.J., Bard, E., Bayliss, A., Beck, J.W., Blackwell, P.G., Bronk Ramsey, C., Grootes, P.M., Guilderson, T.P., Haflidason, H., Hajdas, I., Hatté, C., Heaton, T.J., Hoffmann, D.L., Hogg, A.G., Hughen, K.A., Kaiser, K.F., Kromer, B., Manning, S.W., Niu, M., Reimer, R.W., Richards, D.A., Scott, E.M., Southon, J.R., Staff, R.A., Turney, C.S.M., van der Plicht, J., 2013. IntCal13 and Marine13 radiocarbon age calibration curves 0–50,000 years cal BP. Radiocarbon 55 (4), 1869–1887.
Rhodes, T.E., Gasse, F., Lin, R., Fontes, J.C., Wei, K., Bertrand, P., Gibert, E., Melieres, F., Tucholka, P., Cheng, Z.Y., 1996. A late Pleistocene-Holocene lacustrine record from Lake manas, Zunggar (northern xinjiang, western China). Palaeogeogr. Palaeoclimatol. Palaeoecol. 120, 105–121.
Rodriguez-Iturbe, I., D'odorico, P., Porporato, A., Ridolfi, L., 1999. On the spatial and temporal links between vegetation, climate, and soil moisture. Water Resour. Res. 35 (12), 3709–3722.
Romanovskiy, V.V., 2007. Climate, glaciers and lakes of the tien shan: Journey to the past. Bishkek, Izd. Ilim. 162 (in Russian).
Scholes, R.J., Walker, B.H., 1993. An African Savanna. Cambridge University Press, Cambridge, UK.
Shakun, J.D., Carlson, A.E., 2009. A global perspective on Last Glacial Maximum to Holocene climate change. Quat. Sci. Rev. 29 (15), 1801–1816.
Shi, Y.F., Wen, Q.Z., Qu, Y.G., 1990. Changes in Quaternary Climate Environments and Geohydrological Conditions in Chaiwopu Basin, Xinjiang. Ocean Press, Beijing, p. 15 (in Chinese).
Shi, Y., Shen, Y., Kang, E., Li, D., Ding, Y., Zhang, G., Hu, R., 2007. Recent and future climate change in northwest China. Clim. Change 80, 379–393.
Shichi, K., Takahara, H., Hase, Y., Watanabe, T., Nara, F.W., Nakamura, T., Tani, Y., Kawai, T., 2013. Vegetation response in the southern Lake Baikal region to abrupt climate events over the past 33 cal kyr. Palaeogeogr. Palaeoclimatol. Palaeoecol. 375, 70–82.
Simakova, A.N., 2006. The vegetation of the Russian Plain during the second part of the Late Pleistocene (33–18 ka). Quat. Int. 149, 110–114.
Sun, J.M., Ding, Z.L., Liu, T., 1998. Desert distributions during the glacial maximum and climatic optimum: example of China. Episodes 21, 28–30.
Sun, X.J., Wang, F.Y., Song, C.Q., 1996. Climate response surface from pollen data for part of pollen species in North China. Sci. China. Ser. D-Earth Sci. 26, 431–436 (in Chinese).
Swann, G.E.A., Mackay, A.W., Leng, M.J., Demory, F., 2005. Climatic change in Central Asia during MIS 3/2: a case study using biological responses from Lake Baikal. Glob. Planet. Change 46, 235–253.
Takeuchi, N., Fujita, K., Aizen, V.B., Narama, C., Yokoyama, Y., Okamoto, S., Naoki, K., Kubota, J., 2014. The disappearance of glaciers in the Tien Shan Mountains in Central Asia at the end of Pleistocene. Quat. Sci. Rev. 103, 26–33.
Tang, L.Y., Zhang, Y.P., Zhou, Z.Z., 2012. Morphological variation of Compositae pollen from Quaternary sediments of Eurasia. Acta micropalaeontol. Sin. 51 (1), 64–75 (in Chinese).
Tao, S.C., An, C.B., Chen, F.H., Tang, L.Y., Wang, Z.L., Lü, Y.B., Li, Z., Zheng, T., Zhao, J., 2010. Pollen-inferred vegetation and environmental changes since 16.7 ka BP at Balikun Lake. Xinjiang. Chin. Sci. Bull. 55 (22), 2449–2457.
ter Braak, C.J.F., Šmilauer, P., 2003. Canoco for Windows v.4.52. Biometris, Wageningen, the Netherlands.
Thompson, L.G., Yao, T., Davis, M., Henderson, K.A., Mosley-Thompson, E., Lin, P.-N., Beer, J., Synal, H.A., Cole-Dai, J., Bolzan, J.F., 1997. Tropical climate instability: the Last Glacial cycle from a Qinghai-Tibetan ice core. Science 276, 1821–1825.
Van Campo, E., Cour, P., Hang, S.X., 1996. Holocene changes in Bangong Co basin (Western Tibet). Part 2: the pollen record. Palaeogeogr. Palaeoclimatol. Palaeoecol. 120, 49–63.
Wang, F.X., Qian, N.F., Zhang, Y.L., Yang, H.Q., 1995. Pollen Flora of China. Science Press, Beijing, p. 461 (in Chinese).
Wang, N., Zhao, Q., Li, J., Hu, G., 2003. The sand wedges of the last ice age in the Hexi Corridor, China: paleoclimatic interpretation. Geomorphology 5, 313–320.
Wang, S.M., Dou, H.S., 1998. Chinese Lakes Memoir. Science Press, Beijing, p. 354 (in Chinese).
Wang, W.G., Feng, Z.D., Lee, X.Q., Zhang, H.C., An, C.B., Guo, L.L., 2004. Holocene abrupt climate shifts recorded in Gun Nuur lake core, northern Mongolia. Chin. Sci. Bull. 49, 520–526.
Weltje, G.J., 1997. End-member modeling of compositional data: numerical-statistical algorithms for solving the explicit mixing problem. Math. Geol. 29, 503–549.
Weltje, G.J., Prins, M.A., 2003. Muddled or mixed? Inferring palaeoclimate from size distributions of deep-sea clastics. Sediment. Geol. 162, 39–62.
Williams, M., 2014. Climate Change in Deserts: Past, Present and Future. Cambridge University Press, Cambridge.
Wünnemann, B., Hartmann, K., Janssen, M., Zhang, H.C., 2007. Responses of Chinese desert lakes to climate instability during the past 45,000 years. In: Madsen, D.B., Chen, F.H., Gao, X. (Eds.), Late Quaternary Climate Change and Human Adaptation in Arid China, Developments in Quaternary Science, vol. 9. Elsevier, Amsterdam, pp. 11–24.
Xi, Y.Z., Ning, J.C., 1994. Study on pollen morphology of plants from dry and semidry region. Yushania 11, 119–191.
Xu, Y., Yan, S., Jia, B., Yang, Y., 1996. Numerical relationship between the surface spore/pollen and surrounding vegetation on the southern slope of Tianshan Mountain. Arid. Land Geogr. 19 (3), 24–30 (in Chinese).
Yan, D.D., Wünnemann, B., 2014. Late Quaternary water depth changes in Hala Lake, northeastern Tibetan Plateau, derived from ostracod assemblages and sediment properties in multiple sediment records. Quat. Sci. Rev. 95, 95–114.
Yan, S., Xu, Y., 1989. Spore-pollen association in surface soils in the Altay Mountains, Xinjiang. Arid. Land Geogr. 6, 26–33 (in Chinese).
Yan, S., Mu, G.J., Xu, Y.Q., Zhao, Z.H., 1998. Quaternary environmental evolution of the Lop Nur region, China. Acta micropalaeontol. Sin. 53 (4), 332–340 (in Chinese).
Yang, X., 1991. Geomorphologische Untersuchungen in Trockenräumen NW-Chinas unter besonderer Berücksichtigung von Badanjilin und Takelamagan. Göttinger Geogr. Abh. 96, 1–124.
Yang, X., Scuderi, L.A., 2010. Hydrological and climatic changes in deserts of China since the late Pleistocene. Quat. Res. 73 (1), 1–9.
Yang, X., Zhu, Z., Jaekel, D., Owen, L.A., Han, J., 2002. Late Quaternary palaeoenvironment change and landscape evolution along the Keriya River, Xinjiang, China: the relationship between high mountain glaciation and landscape evolution in foreland desert regions. Quat. Int. 97, 155–166.
Yang, X., Preusser, F., Radtke, U., 2006. Late Quaternary environmental changes in the Taklamakan Desert, western China, inferred from OSL-dated lacustrine and aeolian deposits. Quat. Sci. Rev. 25, 923–932.
Yang, X., Scuderi, L., Paillou, P., Liu, Z., Li, H., Ren, X., 2011. Quaternary environmental changes in the drylands of China – a critical review. Quat. Sci. Rev. 30, 3219–3233.
Yang, X., Wang, X., Liu, Z., Li, H., Ren, X., Zhang, D., Ma, Z., Rioual, P., Jin, X., Scuderi, L., 2013. Initiation and variation of the dune fields in semi-arid China – with a special reference to the Hunshandake Sandy Land, Inner Mongolia. Quat. Sci. Rev. 78, 369–380.
Yang, Z., Kong, Z., Yan, S., Ni, J., Ma, K., Xu, Q., 2004. Pollen distribution in topsoil along the Daxigou Valley in the headwaters of the Urumqi River, the central Tianshan Mountains. Arid. Land Geogr. 27 (4), 543–547 (in Chinese).
Yu, G., Xue, B., Wang, S.M., Liu, J., 2000. Lake-level records of China during the Last Glacial Maximum and its climatic implications. Chin. Sci. Bull. 45 (3), 250–255.
Yu, G., Xue, B., Liu, J., Chen, X., 2003. LGM lake records from China and an analysis of climate dynamics using a modeling approach. Glob. Planet. Change 38 (3), 223–256.
Yu, S.Y., 2015. A Hierarchical Bayesian Model for the Unmixing Analysis of Compositional Data Subject to Unit-sum Constraints. University of New Orleans (Master Thesis).

Zhang, H.C., Wünnemann, B., 1997. Preliminary study on the chronology of lacustrine deposits and determination of high palaeolake levels in Tengger Desert since Late Pleistocene. J. Lanzhou Univ. 33 (2), 87–91.
Zhang, H.C., Li, J.J., Ma, Y.Z., Li, J.J., Qi, Y., Chen, G.J., Fang, H.B., 2001. Late palaeolake evolution and abrupt climate changes during Last Glacial period in NW China. Geophys. Res. Lett. 28 (16), 3203–3206.
Zhang, H.C., Wünnemann, B., Ma, Y.Z., Pachur, H.-J., Li, J.J., Qi, Y., Chen, G.J., Fang, H.B., 2002. Lake level and climate change between 40,000 and 18,000 ^{14}C years BP in Tengger Desert, NW China. Quat. Res. 58, 62–72.
Zhang, H.C., Peng, J.L., Ma, Y.Z., Chen, G.J., Feng, Z.D., Li, B., Fan, H.F., Chang, F.Q., Lei, G.L., Wünnemann, B., 2004. Late Quaternary palaeolake levels in Tengger desert, NW China. Palaeogeogr. Palaeoclimatol. Palaeoecol. 211 (1), 45–58.
Zhao, K.L., Li, X.Q., Dodson, J., Zhou, X., 2013. Climate instability during the last deglaciation in central Asia, reconstructed by pollen data from Yili Valley. NW China Rev. Paleobot. Palynol. 189, 8–17.
Zheng, C.J., 1997. Chorography of Hami. Xinjiang University Press, Urumqi, pp. 92–104 (in Chinese).
Zhou, A.F., Chen, F.H., Wang, Z.L., Yang, M.L., Qiang, M.R., Zhang, J.W., 2009. Temporal change of radiocarbon reservoir effect in Sugan Lake, northwest China during the late Holocene. Radiocarbon 51 (2), 529–535.